PV technologies performance comparison in temperate climates

Niccolò Aste, Claudio Del Pero, Fabrizio Leonforte *

Architecture, Built environment and Construction Engineering – ABC, Politecnico di Milano, Via Bonardi 9, 20133 Milano, Italy

Received 22 April 2014; received in revised form 6 August 2014; accepted 10 August 2014

1. Introduction

The actual performance of PV systems is strongly related to the environmental conditions; in detail, the parameters that most affect energy production are global irradiance, ambient temperature and solar radiation spectrum (Monokroussos et al., 2011; Huld et al., 2010; Strobel et al., 2009; Zinßer et al., 2008). These parameters directly affect the operating conditions of PV modules, with particular reference to cells temperature, which can be identified as one of the major factors affecting electricity production. However, each PV technology reacts differently to the variations of cells operating temperature, according to the temperature coefficient (Makrides et al., 2009): the performance of crystalline silicon modules (c-Si), as is well known, decreases when temperature increases (Radziemska, 2003); on the contrary, modules realized with single or multi-junction amorphous silicon cells (a-Si) are able to improve the electrical performance in high-temperature conditions (Makrides et al., 2012). This effect, which is called *thermal annealing*, allows to recover part of the nominal power initially lost due to *Light Induced Degradation* (*LID*), as a consequence of a prolonged exposure to high temperature (McEvoy et al., 2012). These modules have a strongly site-dependent performance, which is typically difficult to predict in terms of actual energy production.

In such a scenario, it is worth to note that the actual performance of PV modules in outdoor conditions is thus determined by the overlapping of several concurrent effects, which are difficult to differentiate and analyze individually (Fanni et al., 2011; Gottschalg et al., 2003).

* Corresponding author. Tel.: +39 0223999468; fax: +39 0223999469.
E-mail address: fabrizio.leonforte@polimi.it (F. Leonforte).

The aim of this study is the definition and the performance comparison of three main categories of PV modules, made, respectively, of crystalline silicon cells (c-Si), micromorphous silicon cells (a-Si/μc-Si) and heterojunction with intrinsic thin layer (HIT). The first category is the most common all over the world (European Photovoltaic Industry Association, 2010), with a stable and predictable performance over time; the second is an emerging technology at commercial level, with very competitive manufacturing costs (Stannowski et al., 2013; Chopra et al., 2004; Zweibel, 1999), and the third achieves a very high energy conversion efficiency among the PV products for civil uses actually available on the market (Taguchi et al., 2014; Tsunomura et al., 2009).

The paper provides the experimental monitoring and a critical analysis of different representative commercial PV modules, applied at the experimental test facility of the Politecnico di Milano University from January 1 to December 31, 2013. The experimental analysis was carried out in order to evaluate in detail the actual performance of the chosen technologies in a temperate climate, under real operating conditions.

2. Experimental setup

This section describes the experimental setup of the PV test facility used to monitor the selected PV technologies. In detail, the test facility is arranged with mounting structures characterized by a variable tilt angle and oriented with an azimuth angle of 0°. The climatic conditions of the reference context are summarized in Table 1

The PV test facility is equipped with sensors aimed at providing measurements of meteorological and operating parameters, in order to determine the energy performance of the components being tested. All devices are connected to a central data-logging system that stores the measurements at 1-min intervals. The data-monitoring system consists of the equipment described in Table 2.

The DC/AC conversion is operated by a transformerless micro-inverter with MPPT tracker, that allows to monitor each PV module separately. The efficiency curve of the inverter provided by the manufacturer was verified with an experimental data-acquisition campaign performed on a sample PV module. The data obtained are shown in Fig. 1.

During 2013 (January 1 to December 31), a section of the above-described experimental facility was arranged in order to perform a comparative monitoring and investigation on different photovoltaic components, installed with a tilt angle of 30°. The monitoring analysis was focused on the three different PV technologies introduced previously, as discussed more in detail in Section 3. In order to identify any functional or unexpected performance anomalies, two identical PV modules were monitored for each technology.

The comparative analysis between modules of the same technology showed a difference in performance parameters lower than the accuracy of the monitoring devices. For this reason, in the prosecution of the work, only the data related to one module for each technology tested are shown.

A schematic of the described PV test facility section is shown in Fig. 2.

It is important to note that, in order to evaluate the operating performance of the modules, the power and the energy acquisition are provided in AC. However, the inverter efficiency curve allows to calculate analytically the corresponding DC values.

In addition, the reliability of the DC quantities determined with such method was verified by the presence, on one of the available test benches, of current and voltage DC sensors, which are able to acquire the output data from the PV module.

3. Tested technologies

This section describes the average features of the chosen PV technologies adopted for the comparative analysis. In detail, the chosen modules are PV products widely available on the European market, made of crystalline silicon cells (c-Si), micromorphous cells (a-Si/μc-Si) and heterojunction with intrinsic thin layer (HIT) cells, respectively. A description of each technology is provided in the following sub-sections.

3.1. c-Si

The most common PV technology on the market is the crystalline silicon (c-Si). Commercial modules, made of 0.2–0.5 mm thick PV cells, generally connected in series or in parallel, are characterized by an efficiency typically in the range of 11–20% and a temperature coefficient on power between 0.3 and 0.5%/K (Tiwari et al., 2011). Crystalline technology can be divided in multiple categories, according to the crystallinity and crystal size in the resulting wafer. The most used categories are monocrystalline silicon cells (sc-Si) and multicrystalline silicon cells (mc-Si), which have very similar characteristics, although the conversion efficiency of the monocrystalline cells is typically slightly higher. Which is why, in this work, sc-Si technology was considered as representative of the whole category (c-Si).

The cells of the considered module are realized through the well know Czochrahki method (McEvoy et al., 2012).

It is important to note that c-Si PV modules are able to convert solar energy into electrical energy in a wide spectrum, typically between 350 and 1200 nm, with a higher quantum efficiency in the near-infrared band (Sirisamphanwong and Ketjoy, 2012; Ishii et al., 2011; Minemoto et al., 2007).

The modules analyzed are characterized by the parameters summarized in Table 3.

3.2. a-Si/μc-Si

One of the most promising thin-film silicon solar technology is the so-called micromorph tandem, because it combines theoretical high efficiencies, with respect to other thin-films technologies, with very low manufacturing costs.

Table 1
Representative climatic parameters of the reference climatic context.

Site	Latitude	Degree-days	Summer design temp. (°C)	Winter design temp. (°C)	Annual global irrad. on horiz. plane (kW h/m^2 year)	Annual average wind velocity (m/s)
Milan	45°	2404	32	−5	1270	1.7

Table 2
Data-monitoring equipment and accuracy level.

Instrument	Measurement	u.m	N°	Accuracy
Solar irradiance sensor	Solar irradiance on module plane and on horizontal plane	W/m^2	2	±4%
Temperature sensor	Mean surface temperature of PV modules	°C	8	B class (IEC 60751)
External temperature sensor	Environmental temperature	°C	1	B class (IEC 60751)
Power sensor	Electrical power measurement	W	2	±1%

The manufacturing process combines an amorphous silicon (a-Si) top layer over a microcrystalline silicon layer (μc-Si) on a glass substrate. Between the top and the bottom sub-cell an *intermediate reflector*, generally realized with doped silicon oxide layer, deposited by plasma deposition, ensures current continuity between layers.

The top cell absorbs and converts the visible solar spectrum, typically between 250 and 800 nm, while the bottom one is more sensitive to near-IR wavelengths, in the range between 500 and 1000 nm. In addition, the band-gap combination provided by a-Si/μc-Si corresponds approximately to the ideal band-gap combination, with two main benefits: collection problems are negligible and the photons with an energy above the band-gap energy are absorbed from the corresponding sub-cell (McEvoy et al., 2012). However, in actual practice, several problems exist, for example the amorphous top sub-cell suffers from light-induced degradation (Staebler–Wronski effect) and therefore has to be kept as thin as possible, which means that it is not able to absorb enough light (Meier et al., 2002). Furthermore, a tandem cell is subject to current mismatch between the different sub-cells, with a reduction in the module performance (Krishnan et al., 2009). The a-Si/μc-Si modules analyzed are characterized by the parameters summarized in Table 4.

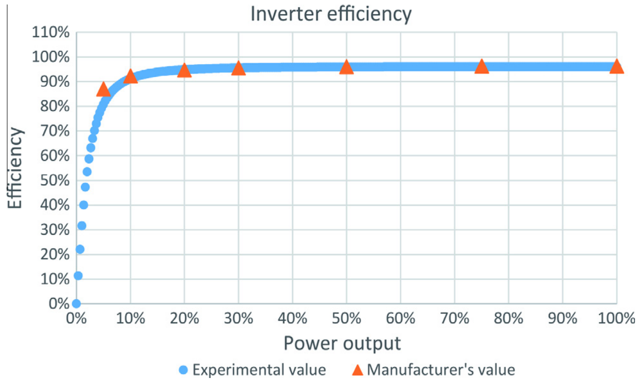

Fig. 1. Micro-inverter efficiency curve.

Table 3
Main features of the c-Si modules tested.

Characteristic	u.m	Value
Area	m^2	1.63
P_{mpp} (STC)	W	250
V_{mpp} (STC)	V	30.6
I_{mpp} (STC)	A	8.17
V_{oc} (STC)	V	37.8
I_{sc} (STC)	A	8.62
NOCT	°C	45
Temperature coefficient on power	%/K	−0.44
Temperature coefficient on V_{OC}	%/K	−0.327
Temperature coefficient on I_{SC}	%/K	0.033

3.3. HIT

The HIT cell, similarly to the tandem cell, combines crystalline and amorphous silicon technology to produce a highly efficient PV module. More in detail, an intrinsic a-Si layer, a doped a-Si layer and a TCO layer are deposited on both sides of a crystalline silicon substrate. The entire manufacturing process requires temperatures lower than 200 °C, which allows to preserve the initial high-level quality of the crystalline silicon substrate.

The sandwich obtained allows to use a wide spectrum of solar radiation, in the range of 350–1100 nm, with conversion efficiencies of the cell up to 22.5% (Taguchi et al., 2014; Tsunomura et al., 2009) and temperature coefficients on power in the order of 0.25–0.3%/K.

The modules analyzed are characterized by the parameters summarized in Table 5.

4. Seasonal performance assessment

As previously mentioned, the modules tested were monitored for one year, from January 1, 2013, to December 31, 2013, with an interruption due to a malfunction on the first 14 days of February.

The first step of the analysis is focused on the evaluation of the modules performance in relation to the seasonal variation. The investigation aims at establishing a correlation

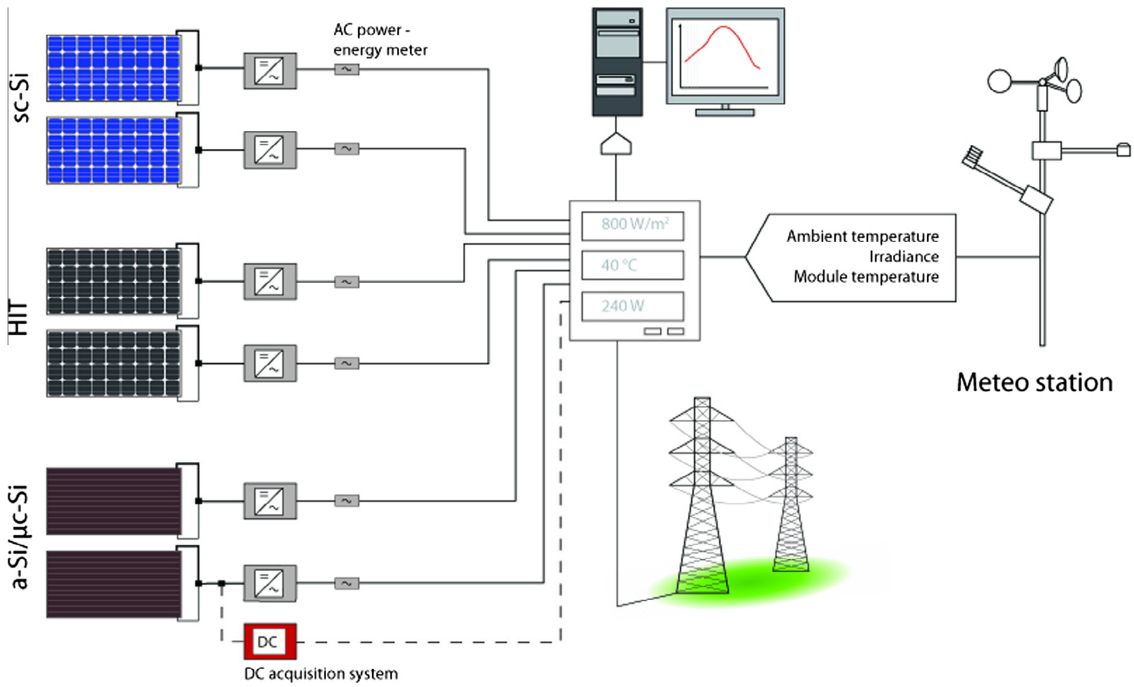

Fig. 2. Schematic of the PV test facility.

between performance and climatic conditions. The experimental results are discussed in the following section.

4.1. Preconditioning of the modules

As is well known, amorphous silicon cells undergo a remarkable degradation process when the PV module is initially exposed to light (*Light Induced Degradation – LID*) (Kenny et al., 2014). The magnitude of this degradation is related to several factors, such as the a-Si layer thickness and the number of junctions, that may account for an initial power reduction between 15% and 35% (Fanni et al., 2011).

The published experimental research showed that the amount of energy needed to consider the amorphous silicon modules as stabilized must be higher than 400–500 kW h/m^2 (Kenny et al., 2014). For such reason, in this work before starting the monitoring phase all the products monitored were exposed, as a precaution, to outdoor conditions for a period of 12 months, corresponding to an irradiation of about 1400 kW h/m^2.

The performance analyses were therefore carried out considering the stabilized power of the monitored PV modules.

4.2. Performance ratio calculation

The PV technologies were analyzed and compared in terms of performance ratio (PR) on energy, normalized for the inverter efficiency. The PR index measures the deviation between the actual performance of a PV system and that theoretically achievable under standard test conditions (STC) and it may be defined as:

$$PR = \frac{E \times I_{stc}}{H \times P} \quad (1)$$

where E (W h) is the output energy generated by the module in the selected time period, I_{stc} is the solar irradiance

Table 4
Main features of the a-Si/µc-Si modules tested.

Characteristic	u.m	Value
Area	m^2	1.42
P_{mpp} (STC)	W	128
V_{mpp} (STC)	V	45.4
I_{mpp} (STC)	A	2.82
V_{oc} (STC)	V	59.8
I_{sc} (STC)	A	3.45
NOCT	°C	44
Temperature coefficient on power	%/K	−0.24
Temperature coefficient on V_{OC}	%/K	−0.30
Temperature coefficient on I_{SC}	%/K	0.07

Table 5
Main features of the HIT modules tested.

Characteristic	u.m	Value
Area	m^2	1.38
P_{mpp} (STC)	W	250
V_{mpp} (STC)	V	34.9
I_{mpp} (STC)	A	7.18
V_{oc} (STC)	V	43.1
I_{sc} (STC)	A	7.74
NOCT	°C	46
Temperature coefficient on power	%/K	−0.3
Temperature coefficient on V_{OC}	%/K	−0.25
Temperature coefficient on I_{SC}	%/K	0.03

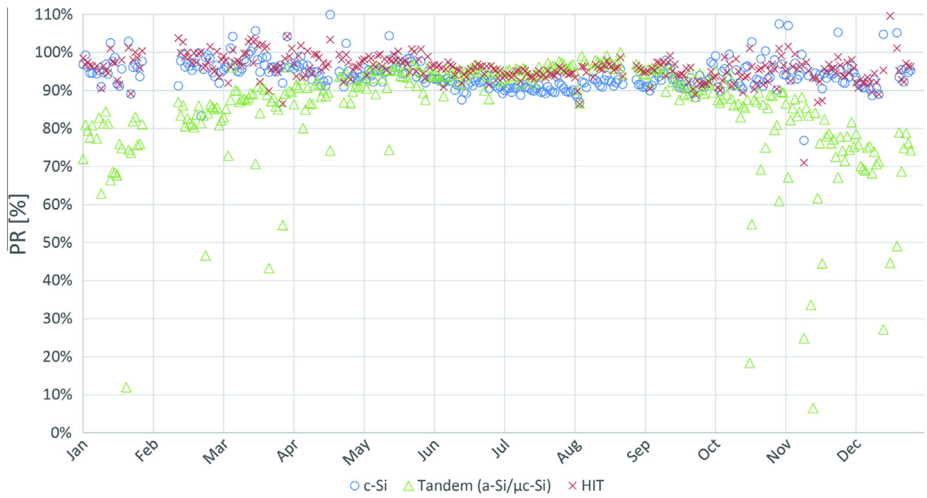

Fig. 3. Daily performance ratio over the monitoring year.

under standard test conditions, *H* is the solar irradiation on the module plane in the selected time (W h/m^2) and *P* (W) is the nominal power of the module measured under standard test conditions.

Fig. 3 shows the average daily *performance ratio* of the three PV technologies tested over the monitoring period.

While the PR of the modules made of c-Si and HIT cells undergoes small fluctuations over the year, with an average annual value of 93% and 96%, respectively, the annual perfor mance of the tandem a-Si/μc-Si technology is slightly lower, quantifiable at a PR of 91%, and a pronounced seasonal variation of the chosen performance parameter was observed.

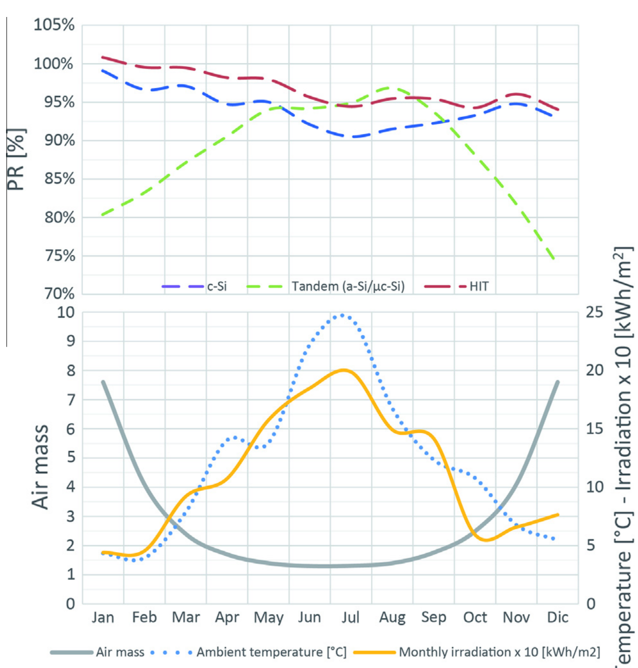

Fig. 4. Average monthly PR, ambient temperature and air mass over the monitoring year (January–December 2013).

In order to perform a more in-depth study of the seasonal variation of each technology monitored, in next sections of the work an assessment of the *performance ratio* related to the climatic conditions was carried out.

4.3. Influence of climatic parameters on energy performance

In order to evaluate the influence of the environmental parameters on the energy performance, three key climatic variables were chosen:

1. Average daily ambient temperature.
2. Daily solar irradiation.
3. Average daily Air Mass (AM).

The first two parameters directly affect the operating temperature of the PV module, according to well-known correlations (Kurnik et al., 2011). It is important to note that, although the wind speed modifies the operating temperature of the PV modules, in the climatic context analyzed such influence factor can be considered negligible.

The Air Mass, instead, is commonly used, in the absence of experimental spectral measurements on solar radiation, as an indicator of the spectral quality of the radiation, although it is not able to predict the spectral variation due to the amount of atmospheric vapor, turbidity or particle pollution (Hisdal, 1987). The AM obtained through geometrical considerations is related to the length of the path of the light through the earth's atmosphere and therefore to a solar spectrum that varies with the height of the sun in the sky. In detail, at low AM values the solar spectrum tends towards the blue wavelength and for higher values of AM the solar spectrum turns to the red band. The performance of different PV modules is related to the variation of AM according to the quantum efficiency of each technology.

The average monthly trends of temperature, irradiation and air mass over the monitoring year and the related PR are shown in Fig. 4.

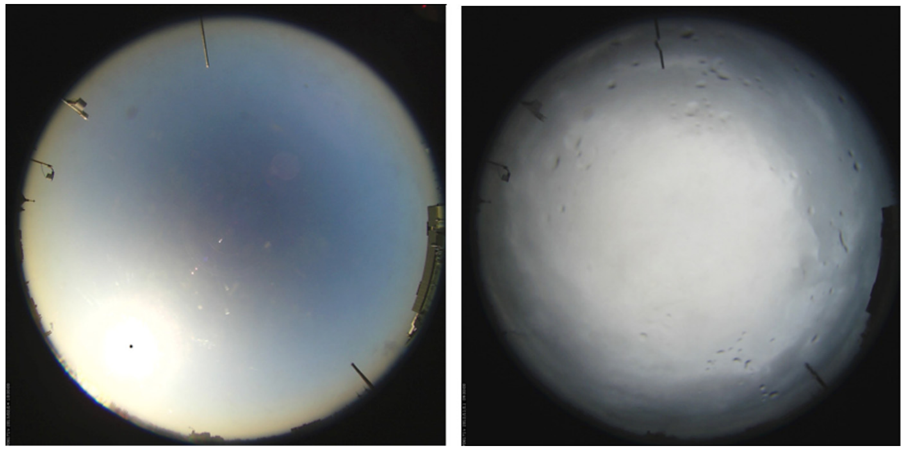

Fig. 5. Fish eye views of clear and overcast sky conditions.

As expected, the PR of the c-Si module decreases when the ambient temperature and the daily irradiation increase; for example, in July, when temperature and irradiation reach their maximum values, the performance ratio of the c-Si technologies reach the minimum average daily value, equal to approximately 90%. On the contrary, PV modules with an amorphous silicon layer (a-Si/μc-Si and HIT) are characterized by low temperature coefficients on power and thus are affected only slightly by the increase of the operating temperature in the hot season.

In addition, the micromorphous silicon module, when subject to high temperatures, is able to recover some of the efficiency initially lost due to *Light Induced Degradation*, achieving during the warmer months a performance higher than the other technologies tested.

In detail, the average monthly performance ratio of tandem technology, during July and August, reaches a peak of 97%.

It is important to note that the thermal effect, known as *thermal annealing*, does not cease when the temperature decreases, but has an hysteresis of about 30 days.

In addition, as is well known and as previously introduced, the spectral composition of the incident solar radiation has a great influence on the seasonal variation of the PR, with particular reference to the products with a layer of amorphous silicon (Virtuani and Fanni, 2014; Gottschalg et al., 2003). Amorphous silicon, in fact, has a narrow spectral response (250–800 nm) and thus is more sensible to the blue components of the spectrum, in comparison with the spectrum response of c-Si (350–1200 nm).

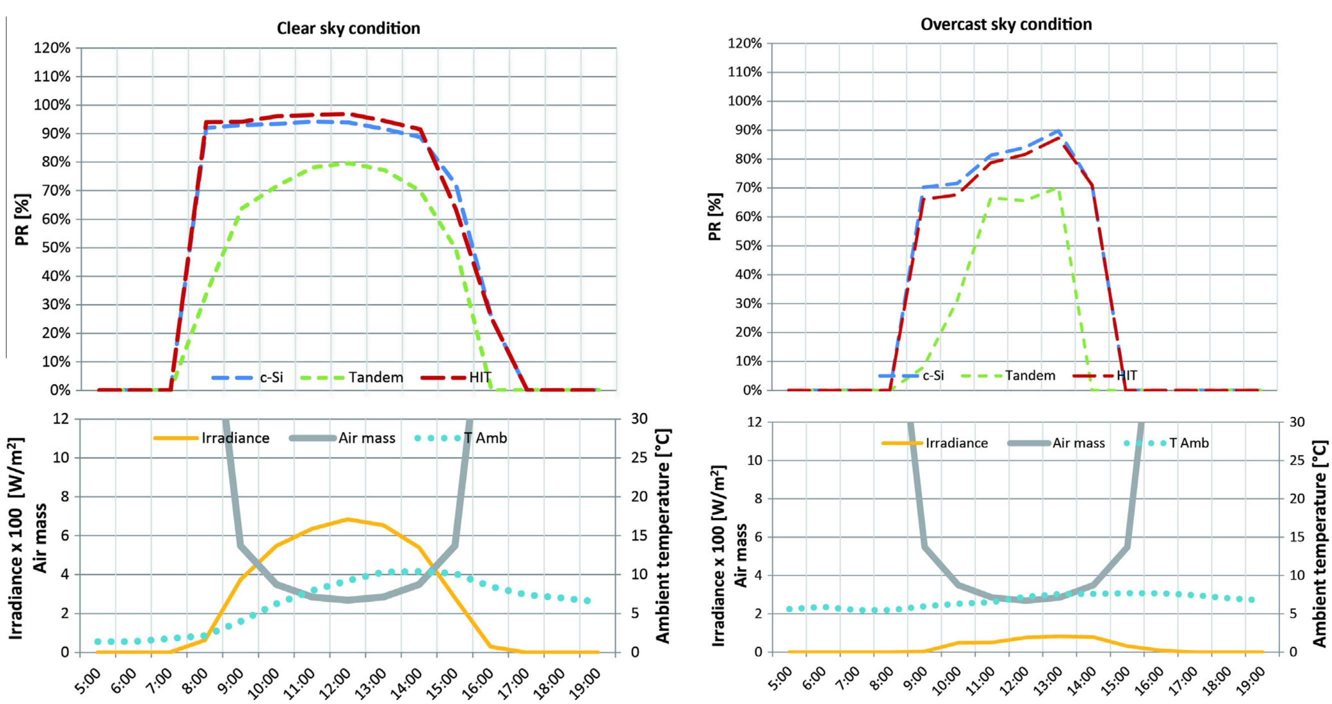

Fig. 6. Hourly PR and climatic data of clear and overcast days in winter (December 2013).

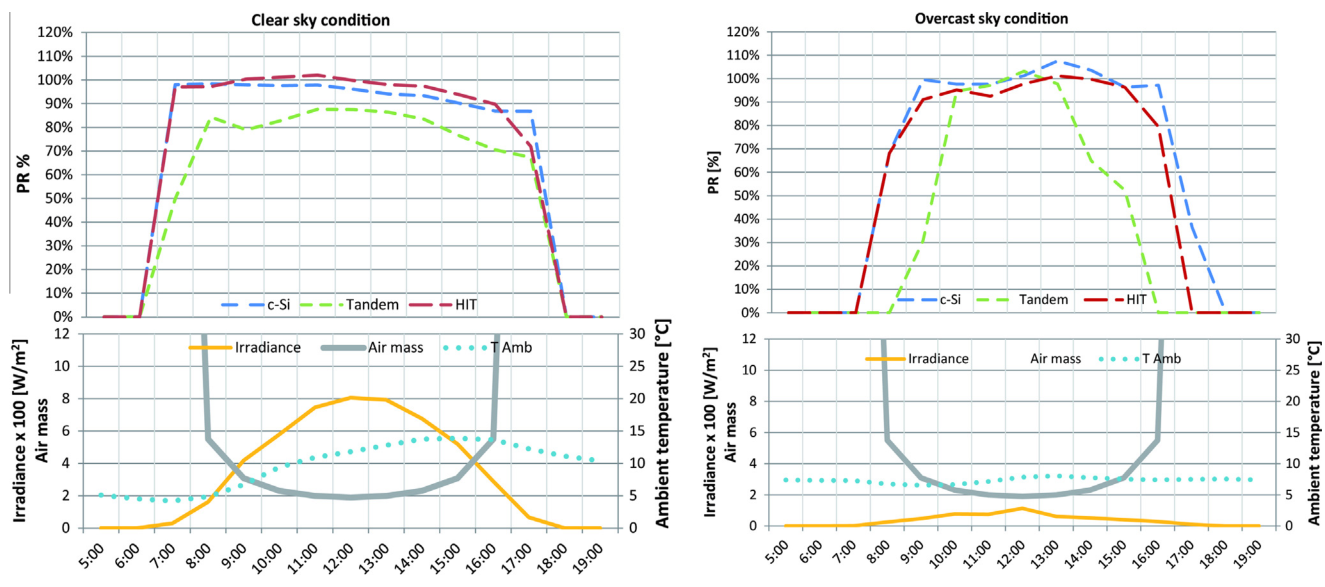

Fig. 7. Hourly PR and climatic data of clear and overcast days in spring (March 2013).

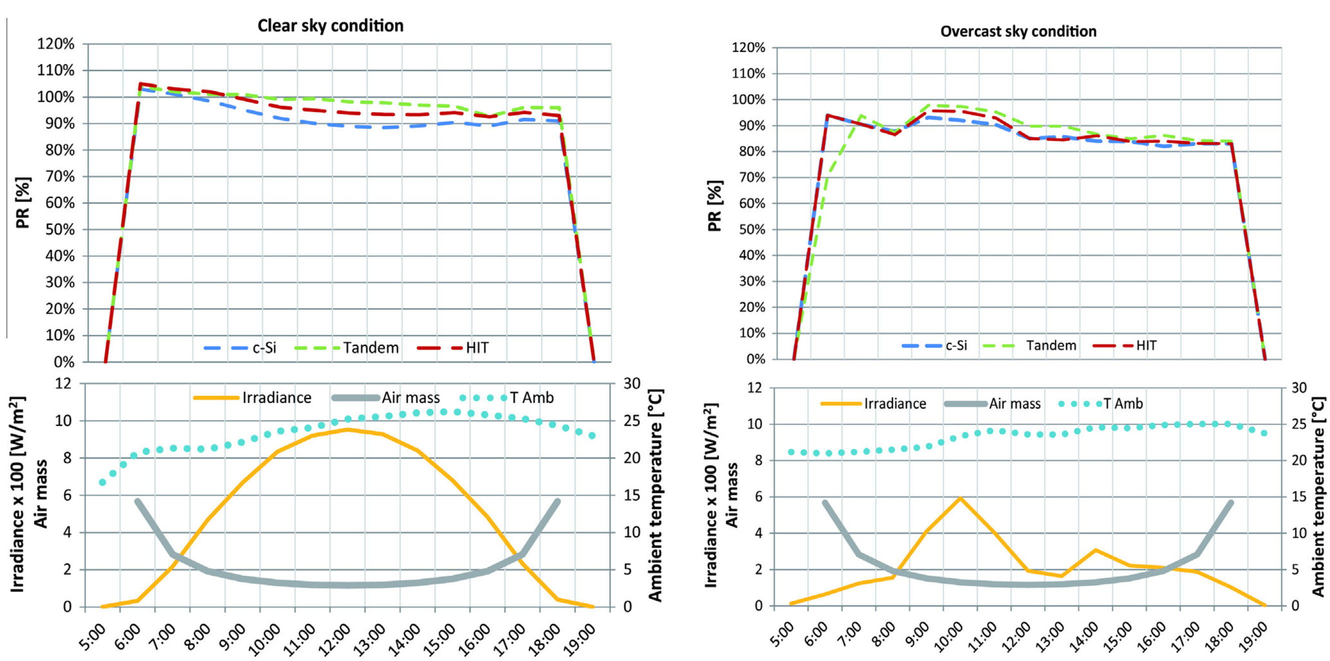

Fig. 8. Hourly PR and climatic data of clear and overcast days in summer (August 2013).

The experimental results confirm that in summer, because the path of the solar radiation passing through the atmosphere is, on average, shorter than in winter, the blue component of sunlight becomes larger and thus the tandem technologies achieves a higher performance value. On this point it is important to note that the *thermal annealing* and the spectral effect overlap over the year and therefore it is quite difficult to clearly distinguish the influence of the two phenomena, due to their similar time phases and partly competitive behavior.

4.4. Daily temperature and spectral influence

To better understand the spectral and thermal effects that affect the final performance of the PV modules monitored, a detailed analysis was carried out on some sample days. The daily analysis is useful, because the incident spectrum can shift significantly toward the red or the blue, both in the course of the day and seasonally (Cornaro and Andreotti, 2013; Nann and Riordan, 1991; Hansen, 1984).

In this sense, in the following figures a PV performance evaluation in clear and overcast sky conditions was reported in three different seasonal period, in December (winter conditions), in March (mid-season) and in August (summer conditions), respectively. The chosen couples of days are selected according to a visual analysis provided by a fish-eye camera installed in the facility. In Fig. 5, samples of clear and overcast sky conditions are shown.

The following charts show and describe the hourly PR of the three technologies analyzed and the climatic parameters previously introduced.

On the analyzed winter and mid-season days of clear sky conditions, shown in Figs. 6 and 7, characterized by an high air mass value and thus by a solar spectrum focused on red, the PR of the tandem module is quite low, with a difference of 10 percentage points compared to the other two technologies considered.

On cloudy days, however, the performance ratio of the tandem module increases during the central hours of the day: it is well known that a thick clouds cover acts as a filter for IR light and shifts the spectrum towards the blue (Green, 1982).

During the clear summer days analyzed, shown in Fig. 8, characterized by high solar irradiance, high ambient temperature values and relatively low AM, the PR of the tandem module achieves better results than that of the c-Si and HIT modules, due to a combination of spectral effect, *thermal annealing* and low temperature coefficient. In particular, while the performances of the c-Si and HIT modules decrease as a function of the temperature, the PV module made of tandem cells maintains the PR almost constant over the day, with peak values equal to approximately 100%.

Under overcast conditions, the three PV technologies have almost the same trend, with slightly higher performance values for the tandem module.

It should be noted that, under overcast conditions, especially in winter, the PV tandem output was very low, and therefore the inverter operated under low input conditions. At low DC input, the inverter did not begin to convert energy, since its threshold energy level was not being met. Nevertheless, the energy lost for such reason during the first and last hours of the day can be considered negligible, it being less than 1%.

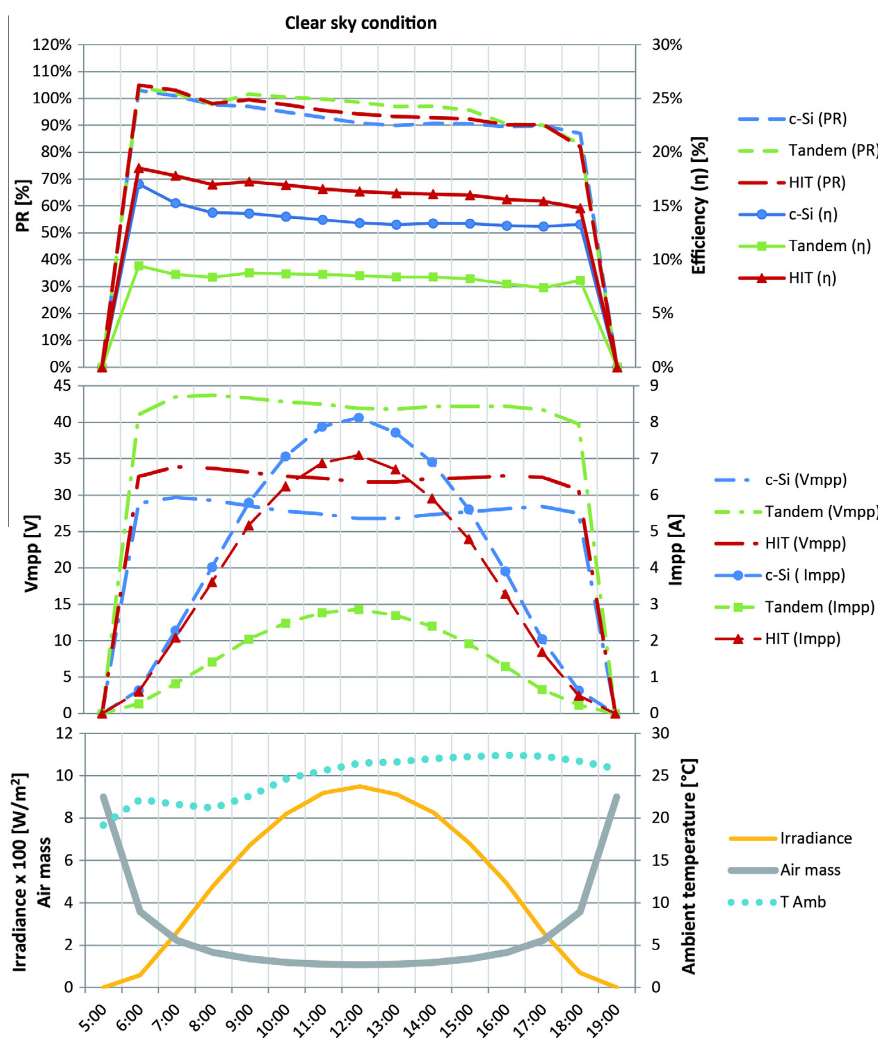

Fig. 9. Hourly parameters variation and climatic data of clear day in summer (July 2014).

Despite PR is one of the main parameters to compare different technologies in real operating conditions, it is also interesting to study in detail the features that contribute to performance definition, such as voltage and current at maximum power point. In fact, as well known, voltage is strongly affected by cells' temperature, while current is mainly related to solar irradiation level. In this sense, the variation of such parameters on a clear sky day in July 2014, that is after 6 months from the end of the monitor campaign, was analyzed and the results are reported in Fig. 9.

As shown, despite the efficiency of the a-Si/μc-Si module is considerably lower compared to the efficiency of c-Si and HIT technologies, in summer period the PR of tandem module achieves higher values than the other analyzed PV modules.

It is interesting to note that, after one year of exposure in actual operating conditions, the performances of the tested modules are substantially equal to those recorded during 2013 in the same period (the difference in daily PR is below 1%).

5. Conclusions

The experimental work presented in this paper provides interesting data, which can be used to assess the performance differences between the three analyzed photovoltaic technologies in operating conditions. The *performance ratio* parameter was chosen in order to compare the PV modules.

The seasonal analysis provides the performance trend over the year: while the performance of the c-Si and HIT modules is rather stable and predictable, the module with an a-Si layer presents widely variable seasonal performance. For this reason, the paper focused on the module with micromorph a-Si/μc-Si silicon cells. In detail, the tandem silicon, sensible to blue light wavelength, is strongly affected by the seasonal solar spectrum, which becomes more red-rich or blue-rich in winter or in summer, respectively, with a corresponding average monthly PR value of 80% in January and 97% in August. However, the amount of radiation available during winter is much lower than in summer; for this reason, the average annual PR of the three technologies is quite similar, with a maximum value for HIT technology (96%), and lower values for the c-Si (93%) and a-Si/μc-Si modules (91%).

In addition to the spectral effects, thermal influence was analyzed: in warmer months micromorphous a-Si/μc-Si silicon cells, in fact, achieve a performance higher than the other technologies tested, due to a low temperature coefficient and *thermal annealing*.

Finally, it was noted that under overcast sky conditions the tandem module increases the performance ratio with an amplitude corresponding to 10% in the spring season.

The observation developed in this paper can be used for the selection of the most suitable PV technology, depending on the climatic conditions.

References

Chopra, K., Paulson, P., Dutta, V., 2004. Thin-film solar cells: an overview. Prog. Photovoltaics Res. Appl. 12, 69–92.

Cornaro, C., Andreotti, A., 2013. Influence of average photon energy index on solar irradiance characteristics and outdoor performance of photovoltaic modules. Prog. Photovoltaics Res. Appl. 21, 996–1003.

European Photovoltaic Industry Association, 2010. Global market outlook for photovoltaics until 2014. <http://www.epia.org/fileadmin/EPIA_docs/public/Global_Market_Outlook_for_Photovoltaics_until_2014.pdf>.

Fanni, L., Virtuani, A., Chianese, D., 2011. A detailed analysis of gains and losses of a fully-integrated flat roof amorphous silicon photovoltaic plant. Sol. Energy 85, 2360–2373.

Gottschalg, R., Infield, D., Kearney, M., 2003. Experimental study of variations of the solar spectrum of relevance to thin film solar cells. Sol. Energy Mater. Sol. Cells 79, 527–537.

Green, M.A., 1982. Solar Cells: Operating Principles, Technology, and System Applications. Englewood Cliffs, NJ, Prentice-Hall Inc. 1982 (288), 1.

Hansen, V., 1984. Spectral distribution of solar radiation on clear days: a comparison between measurements and model estimates. J. Climate Appl. Meteorol. 23, 772–780.

Hisdal, V., 1987. Spectral distribution of global and diffuse solar radiation in Ny-Alesund, Spitsbergen. Polar Res. 5, 1–27.

Huld, T., Gottschalg, R., Beyer, H.G., Topic, M., 2010. Mapping the performance of PV modules, effects of module type and data averaging. Sol. Energy 84, 324–338.

Ishii, T., Otani, K., Takashima, T., 2011. Effects of solar spectrum and module temperature on outdoor performance of photovoltaic modules in round-robin measurements in Japan. Prog. Photovoltaics Res. Appl. 19, 141–148.

Kenny, R.P., Chatzipanagi, A.I., Sample, T., 2014. Preconditioning of thin-film PV module technologies for calibration. Prog. Photovoltaics Res. Appl. 22, 166–172.

Krishnan, P., Schüttauf, J., Van der Werf, C., Houshyani Hassanzadeh, B., van Sark, W., Schropp, R., 2009. Response to simulated typical daily outdoor irradiation conditions of thin-film silicon-based triple-band-gap, triple-junction solar cells. Sol. Energy Mater. Sol. Cells 93, 691–697.

Kurnik, J., Jankovec, M., Brecl, K., Topic, M., 2011. Outdoor testing of PV module temperature and performance under different mounting and operational conditions. Sol. Energy Mater. Sol. Cells 95, 373–376.

Makrides, G., Zinsser, B., Georghiou, G.E., Schubert, M., Werner, J.H., 2009. Temperature behaviour of different photovoltaic systems installed in Cyprus and Germany. Sol. Energy Mater. Sol. Cells 93, 1095–1099.

Makrides, G., Zinsser, B., Phinikarides, A., Schubert, M., Georghiou, G.E., 2012. Temperature and thermal annealing effects on different photovoltaic technologies. Renew. Energy 43, 407–417.

McEvoy, A., Markvart, T., Castaner, L., 2012. Practical Handbook of Photovoltaics: fundamentals and applications, second ed. Academic Press, Waltham, MA.

Meier, J., Dubail, S., Golay, S., Kroll, U., Faÿ, S., Vallat-Sauvain, E., Feitknecht, L., Dubail, J., Shah, A., 2002. Microcrystalline silicon and the impact on micromorph tandem solar cells. Sol. Energy Mater. Sol. Cells 74, 457–467.

Minemoto, T., Toda, M., Nagae, S., Gotoh, M., Nakajima, A., Yamamoto, K., Takakura, H., Hamakawa, Y., 2007. Effect of spectral irradiance distribution on the outdoor performance of amorphous Si// thin-film crystalline Si stacked photovoltaic modules. Sol. Energy Mater. Sol. Cells 91, 120–122.

Monokroussos, C., Bliss, M., Qiu, Y., Hibberd, C., Betts, T., Tiwari, A., Gottschalg, R., 2011. Effects of spectrum on the power rating of amorphous silicon photovoltaic devices. Prog. Photovoltaics Res. Appl. 19, 640–648.

Nann, S., Riordan, C., 1991. Solar spectral irradiance under clear and cloudy skies: Measurements and a semiempirical model. J. Appl. Meteorol. 30, 447–462.

Radziemska, E., 2003. The effect of temperature on the power drop in crystalline silicon solar cells. Renew. Energy 28, 1–12.

Sirisamphanwong, C., Ketjoy, N., 2012. Impact of spectral irradiance distribution on the outdoor performance of photovoltaic system under Thai climatic conditions. Renew. Energy 38, 69–74.

Stannowski, B., Gabriel, O., Calnan, S., Frijnts, T., Heidelberg, A., Neubert, S., Kirner, S., Ring, S., Zelt, M., Rau, B., Zollondz, J.-H., Bloess, H., Schlatmann, R., Rech, B., 2013. Achievements and challenges in thin film silicon module production. Sol. Energy Mater. Sol. Cells 119, 196–203.

Strobel, M.B., Betts, T.R., Friesen, G., Beyer, H.G., Gottschalg, R., 2009. Uncertainty in Photovoltaic performance parameters - dependence on location and material. Sol. Energy Mater. Sol. Cells 93, 1124–1128.

Taguchi, M., Yano, A., Tohoda, S., Matsuyama, K., Nakamura, Y., Nishiwaki, T., Fujita, K., Maruyama, E., 2014. 24.7% Record efficiency HIT solar cell on thin silicon wafer. IEEE J. Photovoltaics 4, 96–99.

Tiwari, G.N., Mishra, R.K., Solanki, S.C., 2011. Photovoltaic modules and their applications: a review on thermal modelling. Appl. Energy 88, 2287–2304.

Tsunomura, Y., Yoshimine, Y., Taguchi, M., Baba, T., Kinoshita, T., Kanno, H., Sakata, H., Maruyama, E., Tanaka, M., 2009. Twenty-two percent efficiency HIT solar cell. Sol. Energy Mater. Sol. Cells 93, 670–673.

Virtuani, A., Fanni, L., 2014. Seasonal power fluctuations of amorphous silicon thin-film solar modules: distinguishing between different contributions. Prog. Photovoltaics Res. Appl. 22, 208–217.

Zinßer, B., Makrides, G., Schubert, M., Georghiou, G., Werner, J.H., 2008. Temperature and intensity dependence of twelve photovoltaic technologies. In: Proceedings of the 23rd European Photovoltaic Solar Energy Conference, pp. 3249–3252.

Zweibel, K., 1999. Issues in thin film PV manufacturing cost reduction. Sol. Energy Mater. Sol. Cells 59, 1–18.